

Uplink Massive MIMO SIR Analysis: How do Antennas Scale with Users?

Tianyang Bai and Robert W. Heath, Jr.
Wireless Networking and Communication Group
The University of Texas at Austin
1616 Guadalupe Street, C0803, Austin, TX 78701
{tybai, rheath}@utexas.edu

Abstract—Massive multiple-input multiple-output (MIMO) is a potential physical layer technology for 5G cellular networks. This paper leverages stochastic geometry to derive the uplink signal-to-interference (SIR) distribution in massive MIMO networks. Based on the derived expressions, a scaling law between the number of base station antennas and scheduled users per cell is provided to preserve the uplink SIR distribution, where the impacts of correlation in small-scale fading and power control in the form of fractional path loss compensation are taken account. Numerical results verify the analysis, and show that fractional power control with a compensation fraction of 0.5 is nearly optimal for the average achievable rate in certain cases.

I. INTRODUCTION

Massive multiple-input and multiple-output (MIMO) is an approach to increase the area spectrum efficiency in 5G cellular systems [1]–[4]. It works by using many antennas in a large-scale antenna array to simultaneously serve a large number of users and provide high sum throughput [1]–[4]. In this paper, we focus on massive MIMO operated in time-division duplex (TDD) mode below 6 GHz, where reciprocity in the channel is exploited to avoid feedback, and pilots are reused to reduce the training overhead [1]–[4]. Prior work showed that due to asymptotic orthogonality between channels, high throughput could be achieved with large-scale antenna arrays through simple signal processing, and that the asymptotic performance of massive MIMO (in the limit of the number of base station antennas) is limited by pilot contamination [1].

Most prior work studied the performance of massive MIMO using a simplified network topology, e.g. considering only a few base stations in a hexagonal grid [1], [5]–[7]. With the densification of cellular networks, it is of interest to consider less regular network topologies with a large number of base stations. Fortunately, simple characterizations of the signal-to-interference ratio (SIR) and rate in large networks were enabled by stochastic geometry [8]. The work in [8], however, does not directly extend to massive MIMO networks, as it focused on the single user per cell scenario with perfect channel state information (CSI). Stochastic geometry was applied to study the asymptotic SIR and rate in a massive MIMO networks in [9], [10], where the asymptotic SIR is shown to be approached with impractically large number of antennas, e.g. 10^4 antennas. Related work in [11] applied stochastic geometry to study the uplink performance under

the identically and independently distributed (IID) fading assumption. A linear scaling between the numbers of base station antennas and scheduled users was found to maintain the same mean interference, which need not preserve the SIR distribution.

In this paper, we apply stochastic geometry to study the uplink SIR performance in a large-scale massive MIMO network using maximum ratio combining (MRC). The proposed model incorporates correlated small-scaling fading with exponential correlation [12], and fractional power control by compensating for a fraction of the path loss as in long term evolution (LTE) systems [13]. Compared with prior stochastic geometry network models [8], the model characterizes the distribution of both inter-cell and intra-cell users in the uplink, and accounts for the effect of imperfect CSI due to pilot contamination. Unlike prior work that focused on the asymptotic performance [9], [10], we derive analytical expressions for the non-asymptotic uplink SIR distribution, as a function of the number of base station antennas and scheduled users per cell. Based on the analytical expressions, the scaling law between the base station antennas and scheduled users per cell is obtained to maintain the same uplink SIR distribution. Our analysis shows that (i) to maintain the same uplink SIR, the number of antennas should generally scale *superlinearly* with the number of scheduled users per cell; (ii) the linear scaling law in [11] preserves the SIR distribution only in the case of full compensation of the path loss in power control; and (iii) correlations in small-scale fading reduce the uplink SIR coverage. Numerical results also indicate that the average per user rate can be maximized by adjusting the compensation fraction in the fractional power control, and the optimal fraction is around 0.5 in certain cases.

II. SYSTEM MODEL

In this section, we introduce the uplink system model for a massive MIMO cellular network operated in the sub-6 GHz band. The model can be extended for massive MIMO at millimeter wave (mmWave) frequencies by incorporating certain differences in propagation and hardware constraints [14]. Each base station is assumed to have M antennas. In each time-frequency resource block, a base station can simultaneously schedule K users in its cell. Let X_ℓ be the location of the ℓ -th base station, $Y_\ell^{(k)}$ be the location of the

k -th scheduled user in the cell of ℓ -th base station, and $\mathbf{h}_{\ell n}^{(k)}$ the channel vector from X_ℓ to $Y_{\ell'}^{(k)}$.

As in [1], we consider a network operated in the following TDD mode with perfect synchronization: in the uplink channel training stage, the scheduled users send their assigned pilots \mathbf{T}_k , and base stations estimate the channels using the orthogonality of the pilots; in the uplink data transmission, the base stations apply MRC to receive the uplink data, based on the channel estimates derived from uplink pilots. Further, we assume full reuse of the orthogonal pilots $\{\mathbf{T}_k\}_{1 \leq k \leq K}$ in the network.

Now, we introduce the channel model assumptions. The channel is assumed to be constant during one resource block and fades independently from block to block. Moreover, we apply a narrowband channel model, as frequency selectivity in fading can be minimized by techniques like orthogonal frequency-division multiplexing (OFDM) and frequency domain equalization [15]. To model the correlated small-scale fading, we express the channel vector as

$$\mathbf{h}_{\ell n}^{(k)} = \left(\beta_{\ell n}^{(k)} \right)^{1/2} \Phi_{\ell n}^{(k)1/2} \mathbf{w}_{\ell n}^{(k)}, \quad (1)$$

where $\beta_{\ell n}^{(k)}$ is the large-scale path loss, $\mathbf{w}_{\ell n}^{(k)}$ is a Gaussian vector with the distribution $\mathcal{CN}(\mathbf{0}, \mathbf{I}_M)$ for Rayleigh fading, and $\Phi_{\ell n}^{(k)}$ is the covariance matrix to account for correlations in small-scale fading. Let $\lambda_{\ell n}^{(k)}[m]$ be the eigenvalues of the covariance matrix $\Phi_{\ell n}^{(k)}$. We assume that for all channels, the trace of the covariance matrix is normalized to M , i.e., $\sum_{m=1}^M \lambda_{\ell n}^{(k)}[m] = M$, and the average square of the eigenvalues is upper bounded by a constant γ :

$$\limsup_{M \rightarrow \infty} \frac{1}{M} \sum_{m=1}^M \lambda_{\ell n}^{(k)2}[m] = \gamma. \quad (2)$$

Note that the constraint in (2) is satisfied by many common channel models, including the IID fading model, the exponential correlation matrix model [12], and the case of uniform linear arrays with certain continuous angular spread [16].

The large-scale path loss gain $\beta_{\ell n}^{(k)}$ is computed as

$$\beta_{\ell n}^{(k)} = C \left(\max \left(R_{\ell n}^{(k)}, \delta \right) \right)^{-\alpha}, \quad (3)$$

where C is a constant determined by the carrier frequency and reference distance, $R_{\ell n}^{(k)}$ is the distance from X_ℓ to $Y_n^{(k)}$, $\alpha > 2$ is the path loss exponent, and $\delta \geq 0$ is a (small) distance, e.g. the reference distance of 1 meter, intended to address the near field effect. Similar path loss models have been used in prior work on cellular network analysis [17, Page 169]. The condition that $\delta > 0$ is essential to prove the convergence of SIR in the asymptotic regime with infinity antennas [14], which requires the finiteness of the path loss. For the analysis in the non-asymptotic regime, we will assume $\delta = 0$ as in [8], [18] for tractability of the analysis.

Next, we introduce the network topology assumptions based on stochastic geometry. We assume the base stations are distributed as a Poisson point process (PPP) with density λ_b .

A user is assumed to be associated with the base station that provides the minimum path loss signal. The users, either scheduled or not in a resource block, are uniformly distributed on the plane with sufficiently high density, such that in any resource block, a base station has at least K candidate users in its cell for potential scheduling. Without loss of generality, a typical scheduled user $Y_0^{(1)}$ is fixed at the origin. We will investigate the SIR and rate performance at this typical user.

Now we focus on the distribution of **scheduled users** in a resource block. For $1 \leq k \leq K$, let $\mathcal{N}_u^{(k)}$ be the point process formed by the locations of the scheduled users $Y_\ell^{(k)}$, i.e., all the scheduled users assigned with the k -th pilot sequence \mathbf{T}_k . Note that even though the users are distributed as a PPP on the plane, the scheduled users do not form a PPP, as their locations are correlated due to the unique assignment of the pilot \mathbf{T}_k within a cell. Unfortunately, the correlations in the scheduled users' locations make the exact analysis intractable [18]. Therefore, we make the following approximations on the distribution of the scheduled user process $\mathcal{N}_u^{(k)}$.

Assumption 1: The following approximations are assumed to model the scheduled users' process $\mathcal{N}_u^{(k)}$:

- 1) The distances $R_{\ell \ell}^{(k)}$ from a user to their associated base stations are assumed to be IID. Note that $R_{\ell \ell}^{(k)}$ is a Rayleigh random variable with mean $0.5\sqrt{1/\lambda_b}$ [8].
- 2) Scheduled users assigned with different pilots are independently distributed, i.e., for $k \neq k'$, the processes $\mathcal{N}_u^{(k)}$ and $\mathcal{N}_u^{(k')}$ are independent.
- 3) The other-cell scheduled users of $\mathcal{N}_u^{(k)}$ are modeled by the *exclusion ball* model [14]: they form a homogeneous PPP with density λ_b outside an exclusion ball centered at the base station X_0 . The radius of the exclusion ball is $\sqrt{1/(\pi\lambda_b)}$.

The assumptions allow for tractable analysis of the SIR and lead to tight approximations as revealed by the simulations in Section IV. In addition, the exclusion ball model can be viewed as the first-order equivalence of the uplink topology model in [18], where the pairwise correlations in users' locations are taken account.

Next, the fractional power control, as used in the LTE systems [13], is assumed in both the uplink training and uplink data stages: the user $Y_\ell^{(k)}$ transmits with power $P_t \left(\beta_{\ell \ell}^{(k)} \right)^{-\epsilon}$, where $\beta_{\ell \ell}^{(k)}$ is the path loss in the desired link, $\epsilon \in [0, 1]$ is the fraction of the path loss compensation, and P_t is the open loop transmit power with no power control. Further, we omit the constraint on the maximum uplink transmit power for simplicity.

To maintain tractability of the analysis using stochastic geometry, we assume that the base stations estimate the channel by correlating the received training signal with the corresponding pilot without using the minimum mean squared error estimation as employed in [6]. Thermal noise is ignored in our analysis, as cellular networks below 6 GHz are mostly interference-limited, and the impact of noise vanishes when the number of antennas M grows large [1]. Hence,

in the channel estimation stage, the estimate of the channel $\mathbf{h}_{\ell\ell}^{(k)}$ at the base station X_ℓ is $\bar{\mathbf{h}}_{\ell\ell}^{(k)} = \left(\beta_{\ell\ell}^{(k)}\right)^{-\epsilon/2} \mathbf{h}_{\ell\ell}^{(k)} + \sum_{\ell' \neq \ell} \left(\beta_{\ell'\ell'}^{(k)}\right)^{-\epsilon/2} \mathbf{h}_{\ell'\ell'}^{(k)}$, where $\sum_{\ell' \neq \ell} \left(\beta_{\ell'\ell'}^{(k)}\right)^{-\epsilon/2} \mathbf{h}_{\ell'\ell'}^{(k)}$ is the estimation error caused by pilot contamination.

In the uplink, to decode the uplink data from $Y_0^{(1)}$, the base station X_0 is assumed to use the channel estimate $\bar{\mathbf{h}}_{00}^{(1)}$ to perform MRC. Therefore, the uplink SIR for the user $Y_0^{(1)}$ is

$$\text{SIR} = \frac{\left(\beta_{00}^{(1)}\right)^{-\epsilon} |\bar{\mathbf{h}}_{00}^{(1)*} \mathbf{h}_{00}^{(1)}|^2}{\sum_{(\ell,k) \neq (0,1)} \left(\beta_{\ell\ell}^{(k)}\right)^{-\epsilon} |\bar{\mathbf{h}}_{00}^{(1)*} \mathbf{h}_{0\ell}^{(k)}|^2}. \quad (4)$$

The proposed system model represents a simple massive MIMO systems in which the SIR expression can be analyzed using stochastic geometry. In the following sections, we will study the uplink SIR distribution.

III. PERFORMANCE ANALYSIS

In this section, we first introduce the asymptotic SIR results, when the number of antennas goes to infinity. Then we focus on the non-asymptotic case with finite base station antennas, where we propose to solve the problem of how the number of antennas M should scale with the number of scheduled users per cell K , to maintain the same uplink SIR.

A. Asymptotic SIR Analysis

Now we study the asymptotic uplink SIR when the number of base station antennas goes to infinity. Similar to the analysis in finite-size networks [1], when $M \rightarrow \infty$, the uplink SIR converges to an asymptotic equivalence in the proposed large-scale networks. The convergence results are summarized in the following theorem. The proof of the results can be found in [14].

Theorem 1: With $\delta > 0$, the uplink SIR in the proposed network converges to its asymptotic equivalence in probability as $\text{SIR}_{\text{UL}} \xrightarrow{p} \frac{\left(\beta_{00}^{(1)}\right)^{2(1-\epsilon)}}{\sum_{\ell \neq 0} \left(\beta_{0\ell}^{(1)}\right)^2 \left(\beta_{\ell\ell}^{(1)}\right)^{-2\epsilon}}$, when the number of antennas $M \rightarrow \infty$. Further, for $\epsilon < 1$, the distribution of the asymptotic SIR can be approximately as

$$\mathbb{P}(\text{SIR} > T) \approx 1 - e^{-\left(\frac{(\alpha-1)}{\Gamma(\epsilon+1)^\alpha}\right)^{\frac{1}{\alpha(1-\epsilon)}}}, \quad (5)$$

where $\Gamma(\cdot)$ is the Gamma function.

Though the asymptotic results provide an upper performance bound for the uplink SIR with finite antennas, however, the tightness of the bound is not guaranteed. As in [10], [14], simulations show that it may require more than 10^4 antennas to approach the asymptotic bound in certain cases. Consequently, we continue to study the non-asymptotic SIR in the subsequent section.

B. SIR Analysis with Finite Antennas

The non-asymptotic SIR for finite base station antennas is generally difficult to analyze, due to the correlation between the interference terms that do not vanish in the non-asymptotic

SIR expression. To obtain insights on the uplink performance, we begin the analysis with the following simple case.

Case 1 (IID fading with no power control): The small-scale fading in all links is assumed to be IID Rayleigh, and the fraction of the path loss compensation is $\epsilon = 0$. In this case, the uplink SIR can be evaluated as follows.

Theorem 2: With IID Rayleigh fading and no fractional power control, the uplink SIR distribution can be approximated as

$$\mathbb{P}(\text{SIR} > T) \approx \sum_{n=1}^N \binom{N}{n} (-1)^{n+1} \int_0^\infty e^{-\mu a_1 t - a_2 t^\alpha} dt, \quad (6)$$

where $\mu = \frac{K}{(M+1)^{2/\alpha}}$, $a_1 = \Gamma(1 - 2/\alpha)(n\eta T)^{2/\alpha} - 1$, $a_2 = \frac{n\eta T}{\alpha-1}$, N is the number of terms used in the approximation, $\eta = N(N!)^{-\frac{1}{N}}$, and $\Gamma(\cdot)$ is the Gamma function.

Proof: See Appendix A. ■

We will show in Section IV that Theorem 2 provides a tight approximation, when $N \geq 5$ terms are used. Moreover, note that in (6), the number of antennas M and the number of scheduled users per cell K only affect the value of μ . Therefore, by Theorem 2, assuming IID fading channel and no power control, the scaling law to maintain the same uplink SIR distribution is $(M+1) \sim K^{\alpha/2}$, which is superlinear when $\alpha > 2$. Next, we extend the results to correlated fading.

Case 2 (Correlated fading with no power control): For the ease of illustration, we use the exponential antenna correlation model [12] as an example to account for the fading correlations, while the results apply to other correlation models satisfying the constraint in (2). In the exponential correlation model [12], the (i,j) -th entry of correlation matrix $\Phi_{\ell\ell'}^{(k)}$ is

$$\Phi_{\ell\ell'}^{(k)}[i,j] = \rho^{|i-j|},$$

where $\rho \in [0, 1]$ is the correlation coefficient of the channels between neighbouring antennas. Measurements showed high correlations, e.g. $\rho > 0.5$, between antennas half-wavelength apart in massive MIMO systems [19]. For simplicity, we assume ρ remains the same for all channels in the analysis. In the correlated fading case, we can compute the uplink SIR in the following corollary.

Corollary 2.1: With correlated fading, the uplink SIR distribution can be approximated via (6) by replacing the scaling constant μ as $\mu = \frac{K\gamma^{2/\alpha}}{(M+2\gamma-1)^{2/\alpha}}$, where γ is the constant defined in (2). Moreover, in the exponential correlation model, γ is computed as $\gamma = \frac{1}{2\pi} \int_0^{2\pi} \left(\frac{1-\rho^2}{1-\rho^2-2\rho \cos(u)} \right)^2 du$.

Proof: See Appendix B. ■

Note that with correlations in fading, the scaling law to preserve the SIR distribution is $(M+2\gamma-1) \sim K^{\alpha/2}$. Compared with the IID fading case, the correlations in fading result in a shift of $2(\gamma-1)$ in the scaling law, which is approximately twice the difference in the average square of the eigenvalues of the fading covariance matrices. Moreover, given the fact that γ increases with ρ , it follows that the higher the correlation, the more antennas are needed to maintain the

same SIR distribution. Next, we continue to study the impact of fractional power control.

Case 3 (Fractional power control): The case with fractional power control is generally difficult to analyze due to the complicated SIR expression. In the case of full path loss compensation ($\epsilon = 1$), where all the scheduled users in a cell have the identical effective path loss after the compensation in power control, the analysis in [6, Corollary 2] show that a linear scaling between M and K is sufficient to keep the SIR unchanged. For general $\epsilon \in (0, 1)$, we can approximate the scaling law between M and K in the following corollary.

Corollary 2.2: With fractional power control, the scaling law between M and K is approximately $(M + 2\gamma - 1) \sim K^s$, where the exponent of the scaling law is $s = \frac{\alpha}{2}(1 - \epsilon) + \epsilon$.

Proof: Note that by [6], when $\epsilon = 1$, $s = 1$, and by Theorem 2, when $\epsilon = 0$, $s = \frac{\alpha}{2}$. Therefore, for general $0 < \epsilon < 1$, the exponent of the scaling law s can be approximated as the linear fitting from the two extreme cases. ■

Though an approximation, the proposed scaling law in Corollary 2.2 matches the simulation results.

Last, we can apply the SIR results to compute the achievable rate. Let the average achievable spectrum efficiency at a typical user be $\xi = \log_2(1 + \min\{\text{SIR}, T_{\max}\})$, where T_{\max} is a SINR distortion threshold determined by the limiting factors like non-linearity in the radio frequency front-end. Given the SIR distribution $\mathbb{P}(\text{SIR} > T)$, the average achievable spectrum efficiency can be computed as in [20, Section III-C].

IV. NUMERICAL RESULTS

In this section, we verify our analytical results with numerical simulations. As a general setup of Monte Carlo simulations, we assume the user density is 60 times the base station density, and the base stations randomly pick K out of the associated users to serve in a resource block. In the simulation, the average inter-site distance between base stations is 300 meters.

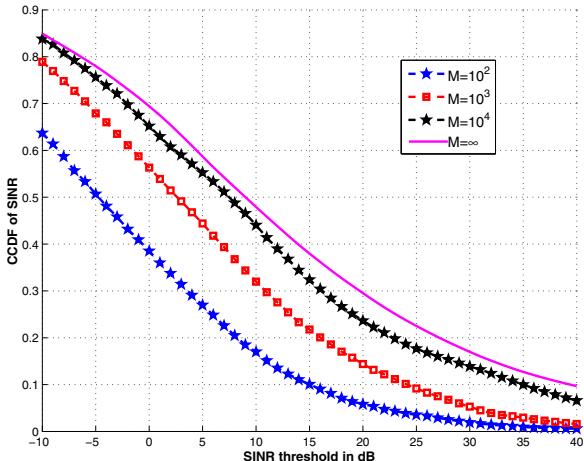


Fig. 1. Convergence to the asymptotic SIR. In the simulations, we assume $\alpha = 4$, $K = 10$, and $\epsilon = 0$. The asymptotic curve is drawn based on Theorem 1.

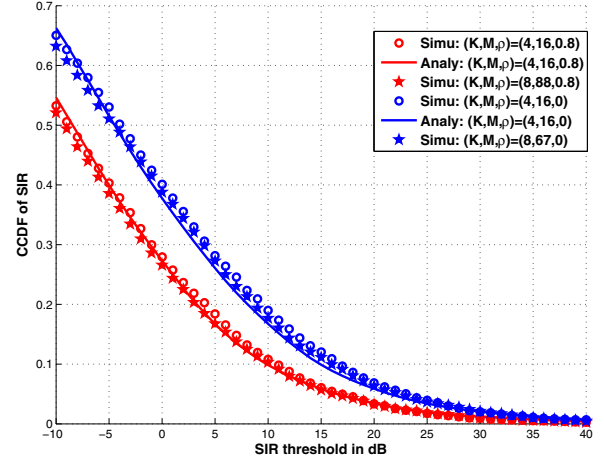


Fig. 2. SIR distributions with correlated fading. We assume $\epsilon = 0$, and $\alpha = 4$. The analytical curves are drawn using $N = 5$ terms, based on Theorem 2 and Corollary 2.1.

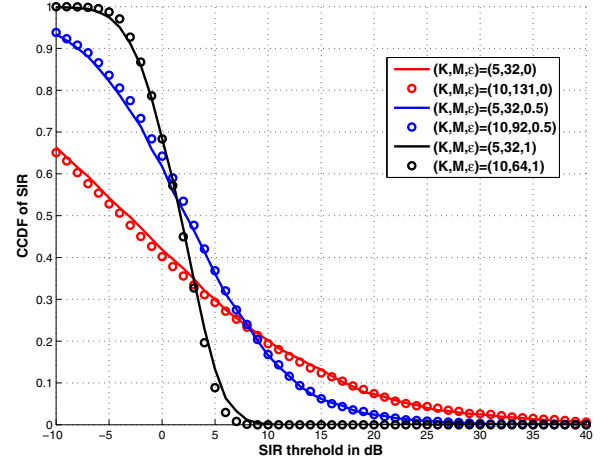


Fig. 3. SIR distributions with fractional power control. We assume $\alpha = 4$, and IID fading channel. Note that $\epsilon = 1$ is for full path loss compensation, and $\epsilon = 0$ for no compensation.

Asymptotic SIR distribution: In Fig. 1, we show the convergence of uplink SIR to its asymptotic equivalence. We assume IID fading channel in the simulations. Numerical results show that more than 10^4 antennas are required to approach the performance in the asymptotic regime.

Impact of fading correlations: We plot the SIR distributions with IID fading and correlated fading in Fig. 2. Note that $\rho = 0$ represents IID fading, and $\rho = 0.8$ indicates high fading correlations. In the simulations, we double the number of scheduled users K from 4 to 8, and scale the number of antennas M according to the proposed scaling laws, which are shown to preserve the SIR distributions in Fig. 2. The impact of correlation can be summarized as follows: (i) correlations in fading degrade the SIR coverage in massive MIMO networks, as fixing M and K , the CCDF of SIR decreases with ρ ; (ii) the correlations requires more antennas than the IID fading case to maintain the uplink SIR when increasing the number

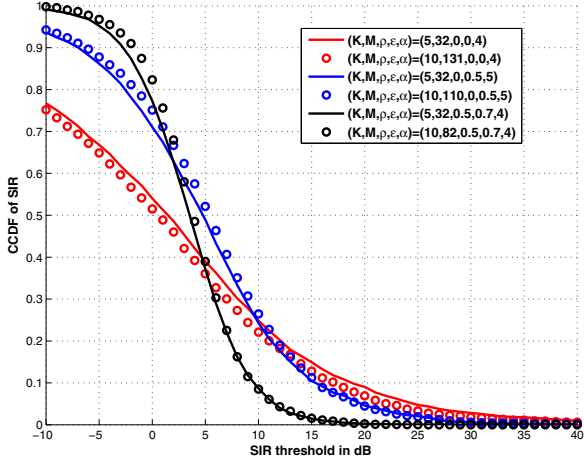


Fig. 4. SIR distribution in the hexagonal grid model. When $K=10$, we compute the required M to preserve the SIR distribution as that of $K=5$, according to Corollary 2.2. Simulations confirm the accuracy of the proposed scaling law.

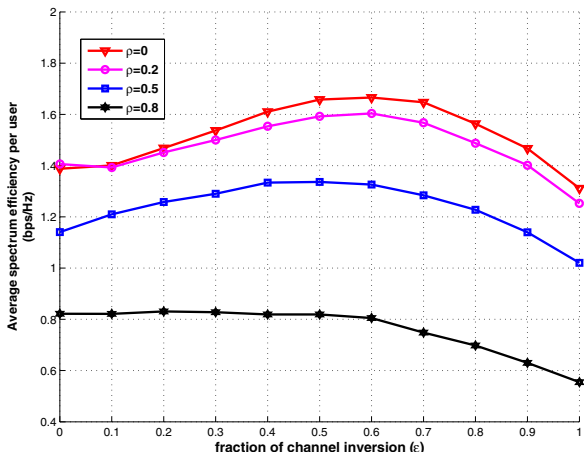


Fig. 5. Average spectrum efficiency per user. In the simulation, we assume $T_{\max} = 21$ dB, which sets the maximum spectrum efficiency per data stream as 7 bps/Hz. Correlations in fading reduce the average spectrum efficiency.

of scheduled users per cell.

Impact of fractional power control: We examine the impact of fractional power control in Fig. 3. We compute the required number of antennas M by Corollary 2.2, when increasing the number of scheduled user K from 5 to 10, and check if the scaling law preserves the SIR distribution by simulations: the proposed scaling law is shown to be accurate in Fig. 3. Numerical results also show that a large compensation fraction ϵ improves the SIR coverage in the low SIR regime at the expense of sacrificing the coverage in the high SIR regime. Intuitively speaking, fractional power control improves the cell-edge user SIR by trading off the performance of the non-cell-edge users.

Verification with hexagonal grid model: In Fig. 4, we use a layout of 19 hexagonal cells with inter-site distance of 300 meters; only the scheduled users in the central cell are counted for the SIR statistics, to avoid edge effect. With

$K = 10$ scheduled users per cell, the required M to maintain the same SIR as that of $(K, M) = (5, 32)$ is computed by Corollary 2.2, which is shown to be almost accurate with extensive combinations of the system parameters in the hexagonal grid model. This shows that the stochastic geometry model provides reasonable predictions even for the hexagonal model.

Rate performance: We illustrate the results on the average spectrum efficiency per user in Fig. 5. In the simulation, we assume $M = 64$ base station antennas, and $K = 10$ scheduled users per cell. Consistent with the SIR results, higher levels of correlations in fading result in lower per user rates. Numerical results also show that the average spectrum efficiency is sensitive to the fraction of the path loss compensation, while the range of the optimum ϵ in the simulations is generally between 0.5-0.6.

V. CONCLUSIONS

In this paper, the uplink SIR in massive MIMO networks with MRC receivers was studied using a stochastic geometry model. Approximate expressions to compute the SIR distributions were derived in both asymptotic and non-asymptotic cases. Based on the SIR analysis, the scaling law between the numbers of antennas and scheduled users per cell was provided to maintain the same uplink SIR distribution. Our analysis showed that compared with the scaling law of IID fading, the spatial correlation resulted in a constant offset in the number of antennas. The exponent of the scaling law is affected by the fractional power control. The analytical results were verified with numerical simulations. Besides, numerical results indicated that the optimum fraction of the fractional power control is roughly 0.5 to maximize the average achievable rate. For future work, the framework can be extended to study the performance of more advanced combining schemes, e.g. with zero-forcing receivers.

APPENDIX

A. Proof of Theorem 2:

First, with M base station antennas, the uplink SIR expression in (4) can be approximated as

$$\begin{aligned} \text{SIR} &\stackrel{(a)}{\approx} \frac{\mathbb{E}|\bar{\mathbf{h}}_{00}^{(1)*}\mathbf{h}_{00}^{(1)}|^2}{\sum_{(\ell,k)\neq(0,1)}\mathbb{E}|\bar{\mathbf{h}}_{00}^{(1)*}\mathbf{h}_{0\ell}^{(1)}|^2} \\ &= \frac{(M+1)\beta_{00}^{(1)2} + \sum_{\ell\neq0}\beta_{00}^{(1)}\beta_{0\ell}^{(1)}}{(M+1)\sum_{\ell\neq0}\beta_{0\ell}^{(1)2} + \sum_{\ell\neq\ell'}\beta_{0\ell}^{(1)}\beta_{0\ell'}^{(1)} + \sum_{k\neq1}\beta_{0\ell}^{(1)}\beta_{0\ell}^{(k)}} \\ &\stackrel{(b)}{\approx} \frac{(M+1)\beta_{00}^{(1)2}}{(M+1)\sum_{\ell\neq0}\beta_{0\ell}^{(1)2} + \beta_{00}^{(1)}\left(\sum_{(\ell,k)\neq(0,1)}\beta_{0\ell}^{(k)}\right)} \\ &\stackrel{(c)}{=} \frac{(M+1)\beta_{00}^{(1)2}}{(M+1)C^2(\pi\lambda_b)^\alpha/(\alpha-1) + \beta_{00}^{(1)}\left(\sum_{(\ell,k)\neq(0,1)}\beta_{0\ell}^{(k)}\right)}, \end{aligned}$$

where in (a) the expectations are taken with respect to the small-scale fading in $\mathbf{h}_{\ell\ell}^{(k)}$; in (b) we drop certain terms that do not scale with M in both the numerator and denominator;

in (c) we approximate $\sum_{\ell \neq 0} \beta_{0\ell}^{(1)2}$ by its mean, which is computed by Campbell's Theorem [21].

Next, conditioning on $R_{00}^{(1)} = x$, we compute the conditional uplink SIR distribution as

$$\begin{aligned} & \mathbb{P}(\text{SIR} > T | R_{00}^{(1)} = x) \\ &= \mathbb{P}\left(1 > T \left(\frac{(\pi\lambda_b)^\alpha x^{2\alpha}}{\alpha - 1} + \frac{x^\alpha (\sum_{(\ell,k) \neq (0,1)} \beta_{0\ell}^{(k)})}{C(M+1)}\right)\right) \\ &\stackrel{(a)}{\approx} \mathbb{P}\left(g > T \left(\frac{(\pi\lambda_b)^\alpha x^{2\alpha}}{\alpha - 1} + \frac{x^\alpha (\sum_{(\ell,k) \neq (0,1)} \beta_{0\ell}^{(k)})}{C(M+1)}\right)\right) \\ &\stackrel{(b)}{\approx} 1 - \mathbb{E}\left[1 - e^{-\eta T \left(\frac{(\pi\lambda_b)^\alpha x^{2\alpha}}{\alpha - 1} + \frac{x^\alpha (\sum_{(\ell,k) \neq (0,1)} \beta_{0\ell}^{(k)})}{C(M+1)}\right)}\right]^N \\ &\stackrel{(c)}{=} \sum_{n=1}^N \binom{N}{n} (-1)^{n+1} e^{-n\eta T \frac{(\pi\lambda_b)^\alpha x^{2\alpha}}{\alpha - 1} - \pi K \lambda_b \Gamma(1-2/\alpha) \left(\frac{n\eta T}{M+1}\right)^{2/\alpha} x^2} \end{aligned}$$

where in (a) we use a “dummy” gamma variable g with unit mean and shape parameter N to approximate the constant number one, and the approximation follows from the fact that g converges to one when N goes to infinity, i.e., $\lim_{n \rightarrow \infty} \frac{n^n x^n - e^{-nx}}{\Gamma(n)} = \delta(x-1)$ [22], where $\delta(x)$ is the Dirac delta function; in (b), the approximation follows from Alzer's inequality [20], [23, Appendix A], where $\eta = N(N!)^{-\frac{1}{N}}$; in (c) we approximate the point process involved with $\sum_{(\ell,k) \neq (0,1)} \beta_{0\ell}^{(k)}$ as a PPP with density $K\lambda_b$, and it follows from computing the Laplacian functional of the homogeneous PPP [21]. Last, noting that $R_{00}^{(1)}$ is a Rayleigh random variable with mean $0.5\sqrt{1/\lambda_b}$ [8], we obtain the uplink SIR distribution by de-conditioning on $R_{00}^{(1)} = x$ and changing the variable as $t = \pi\lambda_b x^2$ ■

B. Proof of Corollary 2.1:

First, similar to the proof in Appendix A, the uplink SIR expression with fading correlations can be approximated as

$$\begin{aligned} \text{SIR} &\approx \frac{\mathbb{E}|\bar{\mathbf{h}}_{00}^{(1)*} \mathbf{h}_{00}^{(1)}|^2}{\sum_{(\ell,k) \neq (0,1)} \mathbb{E}|\bar{\mathbf{h}}_{00}^{(1)*} \mathbf{h}_{0\ell}^{(1)}|^2} \\ &\stackrel{(a)}{\approx} \frac{\frac{M+2\gamma_M-1}{\gamma_M} \beta_{00}^{(1)2}}{\frac{M+2\gamma_M-1}{\gamma_M} \sum_{\ell \neq 0} \beta_{0\ell}^{(1)2} + \beta_{00}^{(1)} \left(\sum_{(\ell,k) \neq (0,1)} \beta_{0\ell}^{(k)}\right)} \\ &\stackrel{(b)}{\approx} \frac{\frac{M+2\gamma-1}{\gamma} \beta_{00}^{(1)2}}{\frac{M+2\gamma-1}{\gamma} \sum_{\ell \neq 0} \beta_{0\ell}^{(1)2} + \beta_{00}^{(1)} \left(\sum_{(\ell,k) \neq (0,1)} \beta_{0\ell}^{(k)}\right)}, \end{aligned}$$

where in (a) $\gamma_M = \frac{\sum_{m=1}^M \lambda_{\ell\ell'}^{(k)2}}{M}$ is the average square of the eigenvalues for the covariance matrix $\Phi_{\ell\ell'}^{(k)}$ in the case of M antennas; in (b) we approximate γ_M with its superior limit γ as defined in (2). Moreover, when assuming the exponential antenna correlation model, the covariance matrices of the fading correlation $\Phi_{\ell\ell'}^{(k)}$ are Toeplitz matrices: by [24], the asymptotic limit of γ_M can be computed as

$\gamma = \frac{1}{2\pi} \int_0^{2\pi} \left(\frac{1-\rho^2}{1-\rho^2 - 2\rho \cos(x)} \right)^2 dx$. The rest of the proof follows the same line as in Appendix A.

ACKNOWLEDGEMENT

This paper is based upon work supported by the National Science Foundation under Grant Nos. 1218338 and 1319556.

REFERENCES

- [1] T. Marzetta, “Noncooperative cellular wireless with unlimited numbers of base station antennas,” *IEEE Trans. Wireless Commun.*, vol. 9, no. 11, pp. 3590–3600, Nov. 2010.
- [2] E. Larsson, O. Edfors, F. Tufvesson, and T. Marzetta, “Massive MIMO for next generation wireless systems,” *IEEE Communications Magazine*, vol. 52, no. 2, pp. 186–195, Feb. 2014.
- [3] L. Lu, G. Li, A. Swindlehurst, A. Ashikhmin, and R. Zhang, “An overview of massive MIMO: Benefits and challenges,” *IEEE J. Sel. Topics Signal Process.*, vol. 8, no. 5, pp. 742–758, Oct. 2014.
- [4] F. Boccardi, R. Heath, A. Lozano, T. Marzetta, and P. Popovski, “Five disruptive technology directions for 5G,” *IEEE Communications Magazine*, vol. 52, no. 2, pp. 74–80, February 2014.
- [5] J. Jose, A. Ashikhmin, T. Marzetta, and S. Vishwanath, “Pilot contamination and precoding in multi-cell TDD systems,” *IEEE Trans. Wireless Commun.*, vol. 10, no. 8, pp. 2640–2651, Aug. 2011.
- [6] J. Hoydis, S. ten Brink, and M. Debbah, “Massive MIMO in the UL/DL of cellular networks: How many antennas do we need?” *IEEE J. Sel. Areas Commun.*, vol. 31, no. 2, pp. 160–171, Feb. 2013.
- [7] H. Yin, D. Gesbert, M. Filippou, and Y. Liu, “A coordinated approach to channel estimation in large-scale multiple-antenna systems,” *IEEE J. Sel. Areas Commun.*, vol. 31, no. 2, pp. 264–273, Feb. 2013.
- [8] J. G. Andrews, F. Baccelli, and R. K. Ganti, “A tractable approach to coverage and rate in cellular networks,” *IEEE Trans. Commun.*, vol. 59, no. 11, pp. 3122–3134, Nov. 2011.
- [9] P. Madhusudhanan, X. Li, Y. Liu, and T. Brown, “Stochastic geometric modeling and interference analysis for massive MIMO systems,” in *Proc. of WiOpt*, May 2013, pp. 15–22.
- [10] T. Bai and R. W. Heath Jr., “Asymptotic coverage probability and rate in massive MIMO networks,” in *Proc. of IEEE Global Conf. on Signal and Information Processing (GlobalSIP)*, Dec. 2014.
- [11] N. Liang, W. Zhang, and C. Shen, “An uplink interference analysis for massive MIMO systems with MRC and ZF receivers,” 2015.
- [12] S. Loyka, “Channel capacity of MIMO architecture using the exponential correlation matrix,” *IEEE Commun. Lett.*, vol. 5, no. 9, pp. 369–371, Sep. 2001.
- [13] W. Xiao et al., “Uplink power control, interference coordination and resource allocation for 3GPP E-UTRA,” in *Proc. of IEEE 64th Vehicular Technology Conference*, Sep. 2006, pp. 1–5.
- [14] T. Bai and R. W. Heath Jr., “Massive MIMO: Millimeter wave or lower frequencies?” *Preprint*, Feb. 2015.
- [15] A. Goldsmith, *Wireless Communications*. Cambridge University Press, 2005.
- [16] A. Adhikary, J. Nam, J.-Y. Ahn, and G. Caire, “Joint spatial division and multiplexing: The large-scale array regime,” *IEEE Trans. on Information Theory*, vol. 59, no. 10, pp. 6441–6463, Oct. 2013.
- [17] F. Baccelli and B. Blaszczyszyn, *Stochastic geometry and wireless networks. Volume II: applications*. NOW publishers, 2009.
- [18] S. Singh, X. Zhang, and J. G. Andrews, “Joint rate and SINR coverage analysis for decoupled uplink-downlink biased cell associations in HetNets,” 2014. [Online]. Available: <http://arxiv.org/abs/1412.1898>
- [19] S. Payami and F. Tufvesson, “Channel measurements and analysis for very large array systems at 2.6 GHz,” in *Proc. of European Conf. Antennas and Propag.*, March 2012, pp. 433–437.
- [20] T. Bai and R. Heath Jr., “Coverage and rate analysis for millimeter-wave cellular networks,” *IEEE Trans. Wireless Commun.*, vol. 14, no. 2, pp. 1100–1114, Feb. 2015.
- [21] F. Baccelli and B. Blaszczyszyn, *Stochastic geometry and wireless networks. Volume I: theory*. NOW publishers, 2009.
- [22] R. Aris, *Mathematical Modeling: A Chemical Engineer's Perspective*. Academic Press, 1999.
- [23] H. Alzer, “On some inequalities for the incomplete Gamma function,” *Mathematics of Computation*, vol. 66, no. 218, pp. 771–778, 1997.
- [24] R. M. Gray, *Toepplitz and Circulant Matrices: A review*. NOW publishers, 2006.